

(NASA-TM-111213) ASSESSMENT OF  
MICROALLOYING EFFECTS ON THE HIGH  
TEMPERATURE FATIGUE BEHAVIOR OF  
NIAL (NASA. Lewis Research Center)  
6 p

N96-17184

Unclas

G3/26 0092361

## ASSESSMENT OF MICROALLOYING EFFECTS ON THE HIGH TEMPERATURE FATIGUE BEHAVIOR OF NiAl

R. D. NOEBE, B. A. LERCH, AND K. BHANU SANKARA RAO\*

NASA Lewis Research Center, Cleveland, OH 44135

\*NRC Associate, NASA-LeRC

### ABSTRACT

Binary NiAl suffers from a lack of strength and poor creep properties at and above 1000 K. Poor creep resistance in turn affects low cycle fatigue (LCF) lives at low strain ranges due to the additional interactions of creep damage. One approach for improving these properties involves microalloying with either Zr or N. As an integral part of a much larger alloying program the low cycle fatigue behavior of Zr and N doped nickel aluminides produced by extrusion of prealloyed powders has been investigated. Strain controlled LCF tests were performed in air at 1000 K. The influence of these microalloying additions on the fatigue life and cyclic stress response of polycrystalline NiAl are discussed.

### INTRODUCTION

It is evident from the substantial research that has been performed on binary NiAl over the years that this intermetallic is deficient as a structural material in at least two areas: low temperature ductility and high temperature strength (1,2). Therefore, any useful structural alloy based on NiAl will contain at least microalloying additions if not macroalloying additions to alter or enhance these critical properties (3,4). The effect of microalloying additions on properties can range quite significantly in NiAl alloys. A few microalloying ( $< 1$  at.%) additions such as Fe and Ga can have a mildly beneficial effect on the tensile ductility of NiAl single crystals (5) but have essentially no impact on the properties of polycrystalline alloys (6). Most other microalloying additions decrease the already limited low temperature tensile ductility and increase the brittle-to-ductile transition temperature of NiAl (2). A number of additions such as Zr, Hf, and Ti, while detrimental to low temperature properties, can have a moderate to very significant strengthening effect at elevated temperatures (2,3,7-9). However, at least one alloying addition, nitrogen, tends to have a mildly positive effect on both the creep resistance (10) and low temperature tensile ductility (11) of polycrystalline NiAl.

Of the various microalloying additions, Zr has been studied in significant detail due to its extremely dramatic impact on the behavior of NiAl. Zr additions decrease the already limited room temperature tensile ductility of polycrystalline NiAl and significantly increase the brittle-to-ductile transition temperature (BDTT) (6,12). The increase in BDTT was attributed to the segregation of Zr to the grain boundaries (13) and the subsequent inhibition of localized deformation mechanisms that are necessary for meeting the Von Mises criterion, and therefore, limiting tensile ductility (14). These deformation studies also indicated that Zr was an extremely potent solid solution strengthening agent. This led to a detailed study of the high temperature deformation behavior of NiAl(Zr) alloys which indicated that even the smallest Zr additions

(0.05 - 0.1 at.%) resulted in alloys that were several times stronger than binary NiAl under identical conditions of temperature and imposed strain rate (9).

However, the effect of Zr or other microalloying additions on the cyclic deformation behavior of NiAl has not been previously investigated. The studies already described would indicate that Zr should have both beneficial and detrimental effects on the cyclic behavior of NiAl. For example, the fatigue life of binary NiAl is superior to most structural materials at 1000 K compared on a plastic strain range basis due to its high ductility (15). Therefore, Zr would tend to reduce this advantage since the ductility of Zr-doped NiAl would be much lower. On the other hand, the fatigue life of NiAl is inferior to superalloys on a stress range basis because of its low flow stress. Zr would probably be beneficial in this regard. In addition, fatigue failure of binary NiAl was attributed to an environmentally assisted fatigue damage mechanism that was aggravated by extensive grain boundary void formation due to creep cavitation (15). Since microalloying additions of Zr are beneficial to both the environmental resistance and creep resistance of NiAl, it should also be good for fatigue resistance. However, the final impact of these competing effects on the cyclic deformation behavior of NiAl are too complicated to predict. Therefore, to further understand the role of microalloying additions on the behavior of NiAl, the 1000 K low cycle fatigue behavior of a NiAl(0.1Zr) alloy prepared by extrusion of prealloyed intermetallic powders was investigated. The results are compared to those of similarly processed binary NiAl and a N-doped NiAl alloy that exhibits a slight improvement in creep strength without the large loss in tensile ductility. Differences in LCF behavior are explained by the basic differences in the deformation behavior of these three powder metallurgy (PM) alloys.

## MATERIALS AND EXPERIMENTAL PROCEDURES

Vacuum atomized powders of stoichiometric NiAl and prealloyed powders of NiAl(Zr) and NiAl(N) were obtained from Homogeneous Metals Inc., Clayville, NY. The chemical compositions of the prealloyed powders are given in Table 1. The nickel aluminide powders were placed in mild steel extrusion cans that were evacuated, sealed air tight, and extruded. Due to the various strengths of the alloys the powders were extruded at different temperatures but all had relatively the same grain size. The parameters employed during extrusion and the average grain size of the three alloys are listed in Table 2.

Cylindrical, dog bone-shaped fatigue samples, 13-mm diameter by 114-mm length, were ground from the extruded rods. The reduced gage section (6.5 mm) of each specimen was electropolished in a solution of 90% methanol-10% perchloric acid at 20-25 volts, 1 amp and 208 K prior to LCF testing. Fully reversed total axial strain controlled LCF tests were conducted at 1000 K ( $\pm 5$  K) in air, in a servohydraulic system equipped with induction heating. Strain was measured using a 13-mm gage length, clip-on, water-cooled extensometer, with alumina probes to allow testing at elevated temperatures. Temperature was measured and controlled by an infrared pyrometer. A constant total strain rate of  $10^{-3} \text{ s}^{-1}$  and a triangular strain-time waveform was employed for the tests conducted over a strain range of 0.2 to 1.2%.

Table 1: Alloy Compositions (at.%).

Alloy	Ni	Al	Zr	N	O	C
NiAl	50.2 $\pm$ 0.2	49.7 $\pm$ 0.2	--	0.0009	0.0250	0.0170
NiAl(N)	50.0 $\pm$ 0.2	49.9 $\pm$ 0.2	--	0.0904	0.0347	0.0057
NiAl(Zr)	49.7 $\pm$ 0.2	50.3 $\pm$ 0.2	0.094	0.0018	0.0324	0.0142

Table 2: Materials Processing Description.

Alloy	Starting Powder	Extrusion Conditions	Grain Size ( $\mu\text{m}$ )
NiAl Heat P2098	Vacuum Atomized -100/+325 Mesh Argon Pressurized	1200 K 12:1	12
NiAl(N) Heat P1810	Vacuum Atomized -100/+325 Mesh Nitrogen Pressurized	1400 K 12:1	18
NiAl(Zr) Heat P1187	Vacuum Atomized -100/+325 Mesh Argon Pressurized	1500 K 12:1	23

## RESULTS

All of the NiAl alloys were fully dense and consisted of equiaxed grains. Fine AlN particles were present in the NiAl(N) alloy (11), otherwise, the microstructure of all three nickel aluminides was quite similar. Table 3 provides the monotonic tensile properties measured for each alloy at 1000 K, along with the monotonic brittle-to-ductile transition temperature (BDTT) based on a strain rate of  $1 \times 10^{-3} \text{ s}^{-1}$ . The low cycle fatigue test temperature was slightly below the BDTT of NiAl(Zr) but much higher than the BDTTs of NiAl and NiAl(N).

Table 3: Mechanical Properties and BDTTs for PM Nickel Aluminide Alloys.

Alloy	Elastic Modulus (GPa)	0.2% Yield Stress (MPa)	UTS (MPa)	Tensile Ductility (%)	Approximate BDTT (K)*
NiAl	126	80	--	>25	630
NiAl(N)	150	94	--	>25	630
NiAl(Zr)	200	320	328	0.3	1120

\*Determined for a strain rate of  $1 \times 10^{-3} \text{ s}^{-1}$ .

The LCF life is plotted versus total strain range in Fig. 1. The total strain fatigue resistance of NiAl(N) was higher than binary NiAl in the range of strain amplitudes examined. Zirconium additions were even more beneficial for fatigue life at total strain ranges below 0.38%. However, on increasing the strain range from 0.38% to 0.40%, the Zr-doped alloy exhibited a drastic reduction in life due to rapid exhaustion of its already limited tensile ductility.

The stress response curves, which represent the locus of peak tensile stresses with successive cycles, are depicted in Fig. 2. There are clear and dramatic differences between the Zr-doped and both the NiAl and NiAl(N) materials. First, NiAl(Zr) displayed much larger response stresses than the other two alloys. Second, NiAl(Zr) exhibited a short period of cyclic hardening and attained a maximum stress in the very early stages of cyclic life. Beyond the maximum stress value, a gradual softening took place prior to a regime of nearly stable stress response. Also, the initial hardening period was prolonged with decreasing strain range. Conversely, NiAl and NiAl(N) experienced cyclic softening initially. This was followed by a period of stable stress response that continued until the tensile stress amplitude decreased rapidly due to the formation of macrocracks and their subsequent growth, which immediately preceded failure. Half-life cyclic

stress-strain curves (Fig. 3) of all the NiAl alloys could be represented by a power law relationship  $\Delta\sigma/2 = K' (\Delta\epsilon_p/2)^n$ , where  $K'$  and  $n'$  are the cyclic strength coefficient and cyclic hardening exponent, respectively. Zr-doping significantly improved cyclic strength and led to a high  $n'$ , while the effect of nitrogen was only marginal on these properties.

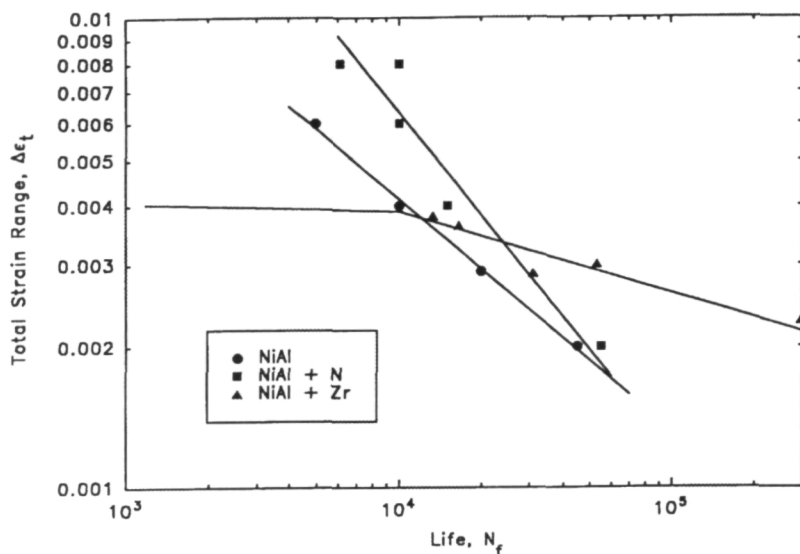


Fig. 1. Fatigue life versus total strain range for PM nickel aluminide alloys at 1000 K.

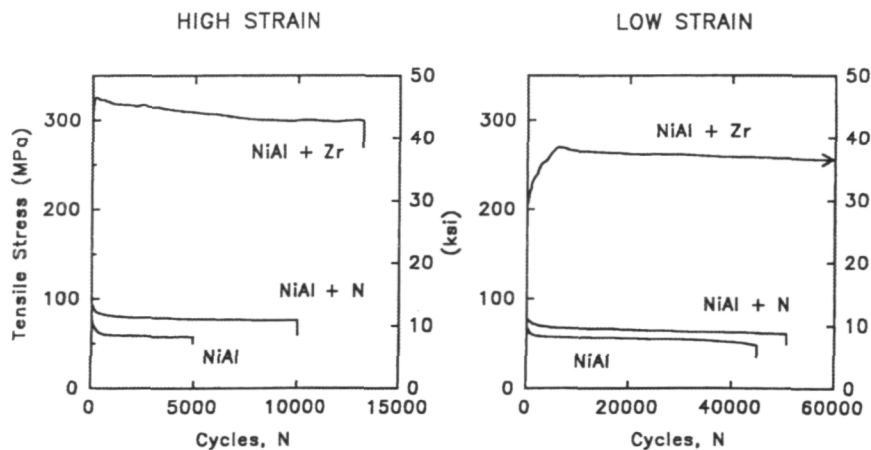


Fig. 2. Typical stress response curves for PM NiAl alloys at high and low strain ranges.

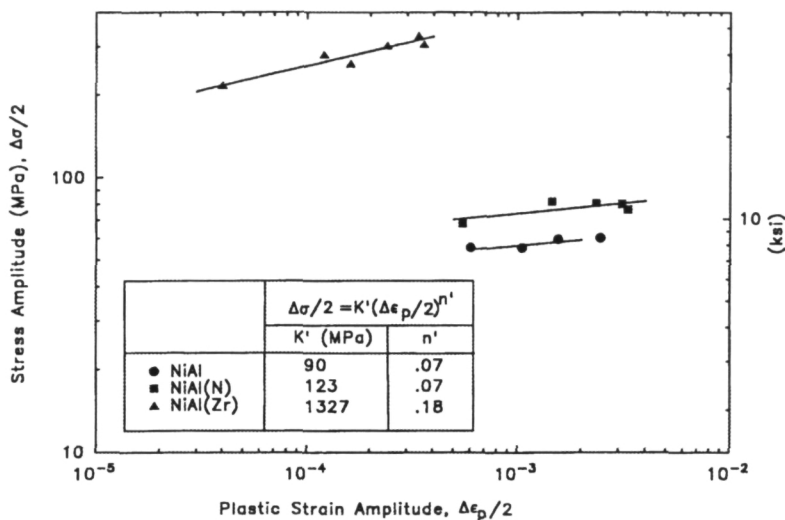


Fig. 3. Cyclic stress-strain curves for PM NiAl alloys at 1000 K.

## DISCUSSION

The low cycle fatigue behavior of the three NiAl alloys is heavily influenced by the relation between test temperature and their respective BDTTs. For NiAl(Zr), the test temperature was just below its BDTT, therefore, recovery was not significant, and this led to the higher and more homogeneous dislocation structure that was observed within the grains (16). Additionally, Zr atoms are very effective in pinning dislocations below the BDTT (12-14) and increasing the viscous drag force on dislocations at higher temperatures (9). Consequently, the mutual interactions between dislocations and the solid solution hardening due to the Zr atoms resulted in significantly higher cyclic stresses and a high  $n'$ . Because the BDTT of the binary and N-doped alloys was much lower than the test temperature, significant recovery was able to occur during testing resulting in a lower  $n'$ . The marginal improvement in cyclic stress response and  $n'$  of the N-doped alloy over the binary NiAl is assumed to be the result of dislocation pinning by the finely dispersed AlN particles in the former alloy.

The two stages in the total strain-life plot of NiAl(Zr) occurred as a result of the change in fracture behavior from slow and stable intergranular crack growth at strain ranges  $\leq 0.38\%$  to brittle cleavage-dominated overload fracture at larger strain ranges. At strain ranges above  $0.38\%$ , the peak tensile stress reached the monotonic cleavage stress of the Zr-doped alloy (328 MPa) in less than 100 cycles, enabling fast crack growth by transgranular cleavage (16). At total strain ranges  $\leq 0.38\%$ , the peak tensile cyclic stresses remained at a much lower level than the cleavage fracture stress. In general, fatigue lives are governed by the ductility of the material at high strains and by its strength at low strains. The longer lives of NiAl(Zr) at low strain ranges result from its basic capacity to resist the applied strains on the basis of high strength. Both the NiAl and NiAl(N) have shorter lives at low strain ranges due to the synergistic interaction between fatigue and creep. A higher slope for the strain range-life plot of the NiAl(N) reflects

this interaction. In order to improve the fatigue resistance of the binary and N-doped alloy, the grain boundaries need to be strengthened to reduce grain boundary sliding and the associated intergranular wedge cracking that was observed in these two alloys. Since Zr segregates to the grain boundaries in NiAl (13) and apparently strengthens the boundary regions preventing grain boundary sliding, NiAl(Zr) does not suffer from this same problem as the other two PM alloys.

## CONCLUSIONS

There were only very minor differences in the fatigue behavior of binary NiAl and NiAl(N) alloys. However, Zr additions significantly altered the fatigue behavior of NiAl at 1000 K. The Zr additions led to a change in the basic deformation behavior of the material such that the fatigue test temperature was just below the BDTT of the alloy instead of significantly above the BDTT as in the other two PM alloys. Zr also increases the tensile flow stress and results in higher response stresses under strain controlled cyclic loading. Furthermore, Zr segregates to the grain boundaries and prevents intergranular sliding and as a consequence increases the fatigue life of the alloy at low strain ranges where the interactions between creep, fatigue and oxidation control life. However, at higher strain ranges the cyclic response stresses quickly exceed the cleavage strength of the alloy resulting in significantly shortened fatigue lives.

## REFERENCES

1. D.B. Miracle, *Acta Metall. Mater.* **39**, 649 (1993).
2. R.D. Noebe, R.R. Bowman and M.V. Nathal, *Inter. Mater. Rev.* **38**, 193 (1993).
3. R. Darolia, *JOM* **43**(3), 44 (1991).
4. C.T. Liu and K.S. Kumar, *JOM* **45**(5), 38 (1993).
5. R. Darolia, D. Lahrman and R.D. Field, *Scripta Metall. Mater.* **26**, 1007 (1992).
6. R.D. Noebe and M.K. Behbehani, *Scripta Metall. Mater.* **27**, 1795 (1992).
7. I.E. Locci, R. Dickerson, R.R. Bowman, J.D. Whittenberger, M.V. Nathal, and R. Darolia, in High Temperature Ordered Intermetallic Alloys V, eds. I. Baker et al., Vol. 288, Materials Research Society, Pittsburgh, PA, pp. 685-690 (1993).
8. W.S. Walston, R.D. Field, J.R. Dobbs, D.F. Lahrman, and R. Darolia, in International Symposium on Structural Intermetallics, eds. R. Darolia et al., TMS, Warrendale, PA, pp. 523-532 (1993).
9. J.D. Whittenberger and R.D. Noebe, submitted to *Metall. Mater. Trans. A*, (1995).
10. J.D. Whittenberger, R.D. Noebe and D.R. Wheeler, to be published in High Temperature Ordered Intermetallic Alloys VI, eds. J. Horton et al., Materials Research Society, Pittsburgh, PA, (1995).
11. R.D. Noebe and A Garg, *Scripta Metall. Mater.* **30**, 815 (1994).
12. R.R. Bowman, R.D. Noebe, S.V. Raj and I.E. Locci, *Metall. Trans. A* **23A**, 1493 (1992).
13. M.V. Zeller, R.D. Noebe and I.E. Locci, in HITEMP Review - 1990, NASA CP-10051, pp. 21-1 to 21-17 (1990).
14. R.D. Noebe, NASA TM-106534, April 1994.
15. B.A. Lerch and R.D. Noebe, *Metall. Mater. Trans. A* **25A**, 309 (1994).
16. K.B.S. Rao, B.A. Lerch and R.D. Noebe, in HITEMP Review - 1994, NASA CP-10146, pp. 53-1 to 53-11 (1994).